Toxicology in Vitro 79 (2022) 105290

Contents lists available at ScienceDirect

Toxicology in Vitro

journal homepage: www.elsevier.com/locate/toxinvit

In vitro and in silico study on consequences of combined exposure to the food-borne alkenylbenzenes estragole and safrole

Shuo Yang [*,1], Tomoyuki Kawai [2], Sebastiaan Wesseling, Ivonne M.C.M. Rietjens

Division of Toxicology, Wageningen University, Stippeneng 4, 6708 WE Wageningen, the Netherlands

ARTICLE INFO

Editor: Dr. Jennings

Keywords:
Combination exposure
Dose addition
Interactions
DNA adduct formation
Cytotoxicity
Alkenylbenzenes

ABSTRACT

Potential consequences of combined exposure to the selected food-borne alkenylbenzenes safrole and estragole or their proximate carcinogenic 1′-hydroxy metabolites were evaluated in vitro and in silico. HepG2 cells were exposed to 1′-hydroxyestragole and 1′-hydroxysafrole individually or in equipotent combination subsequently detecting cytotoxicity and DNA adduct formation. Results indicate that concentration addition adequately describes the cytotoxic effects and no statistically significant differences were shown in the level of formation of the major DNA adducts. Furthermore, physiologically based kinetic modeling revealed that at normal dietary intake the concentration of the parent compounds and their 1′-hydroxymetabolites remain substantially below the Km values for the respective bioactivation and detoxification reactions providing further support for the fact that the simultaneous presence of the two carcinogens or of their proximate carcinogenic 1′-hydroxy metabolites may not affect their DNA adduct formation. Overall, these results point at the absence of interactions upon combined exposure to selected food-borne alkenylbenzenes at realistic dietary levels of intake.

1. Introduction

Via the diet, humans can be exposed to combinations of numerous substrates that may act individually, additively or interactively (synergism and antagonism) with respect to biological effects (Dale and Garner, 1996). In 2012, the EU Scientific Committees on Health and Environmental Risks (SCHER), on Emerging and Newly Identified Health Risks (SCENIHR), and on Consumer Safety (SCCS), emphasized that effects induced by combined exposure could be greater than those induced by the individual compound exposure (Scientific Committee on Consumer Safety, S, et al., 2012). Based on the underlying mode of action, combined exposure may result in i) dose (concentration) addition in case of a similar mode of action at the same target site, ii) response addition for different modes of action, or iii) interaction among compounds resulting in synergism or antagonism, where the total effect of combined exposure to these compounds differs from what is predicted by either response addition or dose (concentration) addition (Bliss, 1939; Howard and Webster, 2009; Staal et al., 2007). However, additional aspects may have to be considered, for instance, compounds with a similar mode of action can also interact with each other via influences on metabolism or induction of metabolic enzymes leading to outcomes different from dose addition (Staal et al., 2007; Lévay and Bodell, 1992).

The current study focuses on the combined effects of two selected model compounds of the group of food-borne alkenylbenzenes. Alkenylbenzenes are substances naturally occurring, often in combination, in different herbs and species. The compounds are of concern because they are genotoxic carcinogens (Miller et al., 1983) and risk assessment can therefore be based on the so-called margin of exposure (MOE) approach (EFSA, 2012). In previous risk assessments by the MOE approach combined exposure to alkenylbenzenes was taken into account assuming dose addition (Alajlouni et al., 2016; Alajlouni et al., 2017; Al-Malahmeh et al., 2017). This assumption was based on the fact that the alkenylbenzenes of interest act on the same target tissue (liver) and via a similar mode of action. Their bioactivation is initiated by cytochromes P450 resulting in conversion of the parent compound to the proximate carcinogenic 1′-hydroxymetabolite, which is subsequently sulfated by sulfotransferases to produce the ultimate carcinogenic 1′-sulfooxymetabolite responsible for the DNA adduct formation. However,

* Corresponding author.
E-mail address: shuoyang0117@163.com (S. Yang).
[1] Current address: Institution of Food Safety and Quality, University of Shanghai for Science and Technology, Jungong Road, 200093, YangPu District, Shanghai, China.
[2] Current address: Food Safety and Consumer Affairs Bureau, Ministry of Agriculture, Forestry and Fisheries, 1-2-1, Kasumigaseki, Chiyoda-ku, Tokyo 100-8950, Japan.

https://doi.org/10.1016/j.tiv.2021.105290
Received 22 June 2021; Received in revised form 20 November 2021; Accepted 28 November 2021
Available online 30 November 2021

further evidence to support the assumed dose addition has not been available. Therefore, the aim of the present study was to study the effects of combined exposure to two model alkenylbenzenes, estragole and safrole. Experimental studies were performed with the 1′-hydroxy metabolites since these were proven to result in measurable cytotoxicity and DNA adduct formation in the HepG2 cells used for the studies (Yang et al., 2020a). Previous studies have shown the essential role of sulfotransferases in the DNA adduct formation, mutagenicity and tumor induction by the alkenylbenzenes (Boberg et al., 1983; Wiseman et al., 1987; Herrmann et al., 2012; Honda et al., 2016), and also that in HepG2 cells sulfotransferase activity is essential and sufficiently active to support formation of the DNA adducts (Yang et al., 2020a; Jeurissen et al., 2008). The latter follows from the fact that exposure of the HepG2 cells to 1′-hydroxyestragole in the presence of the specific sulfotransferase inhibitor pentachlorophenol reduced estragole DNA adduct formation by 90% (Jeurissen et al., 2008). Thus, HepG2 cells contain sufficient sulfotransferase for the bioactivation of the 1′-hydroxy metabolites, and inducing the DNA adduct formation. Potential interactions at the level of the cytochrome P450 mediated 1′-hydroxylation of the parent alkenylbenzenes were evaluated by comparing physiologically based kinetic modeling based predictions of liver concentrations at realistic dietary dose levels to known kinetic constants for these conversions.

2. Material and method

2.1. Chemicals and reagents

Bovine spleen phosphodiesterase II (SPDE II), venom phosphodiesterase I (VPDE I), nuclease P1, phosphatase alkaline (AP), tris(hydroxymethyl)aminomethane (Tris), 3-(4,5-dimethyl-2-thiazolyl)-2,5-diphenyl-2H-tetrazolium bromide (MTT), and ethylenediaminetetraacetic acid (EDTA) were obtained from Sigma (St. Louis, Missouri, USA). Phosphate buffered saline (PBS) (pH 7.4) and Non-Essential Amino Acids (NEAA) were purchased from Gibco (Paisley, UK). Minimum Essential Medium (MEM), L-glutamine, and penicillin-streptomycin (P/S) were purchased from Gibco (Grand Island, New York, USA). Fetal Bovine Serum (FBS) was purchased from Bodinco BV (Alkmaar, Netherlands). Dimethylsulfoxide (DMSO), hydrochloric acid (HCl), zinc sulfate ($ZnSO_4$), and sodium acetate were purchased from Merck (Darmstadt, Germany). Acetonitrile (ACN) was purchased from Biosolve (Dieuze, France). RNeasy Lysis buffer (RLT) was purchased from QIAGEN (Hilden, Germany). Formic acid was purchased from VMR (Fontenay-sous-Bois, France). 1′-hydroxyestragole (1'-OH estragole) and 1′-hydroxysafrole (1'-OH safrole) were synthesized as described previously (Paini et al., 2010).

2.2. Cell model

HepG2 cells were obtained from the American Type Culture Collection (Manassas, Virginia, USA) and cultured with MEM supplemented with 10% (*v*/v) FBS, 1% (v/v) P/S mixture with L-glutamine and 1% (v/v) NEAA and incubated at 37 °C in a humidified 5% CO_2 atmosphere. The culture medium was refreshed every two or three days until the cell density reached 80%. The cultured cells were either seeded in 96-well plates (Greiner Bio-One, Frickenhausen, Germany) for cytotoxicity experiments or in T-25 flasks (Greiner Bio-One, Frickenhausen, Germany) for experiments on DNA adduct formation.

2.3. Cytotoxicity

HepG2 cells were seeded in 96-well plates at the concentration of 2 $\times$ 10^4 cells/well for one day growth and exposed to 1'-OH estragole or 1'-OH safrole individually or in combination in serum-free medium for 24 h. For the individual exposure, the concentrations were 0, 30, 50, 70, 100, and 150 μM for 1'-OH estragole, and 0, 100, 200, 400, 800 and 1000 μM for 1'-OH safrole. For the combined exposure, 1'-OH estragole was chosen as the reference compound. Therefore, the relative potency factor (RPF) was defined as 1.00 for 1'-OH estragole. The RPF for 1'-OH safrole was derived from the cytotoxicity experiments with the individual compounds and used to define equipotent mixtures for the combined exposure experiments. A series of mixture concentrations in the range between 0 μM and 150 μM 1'-OH estragole equivalents was tested. The final concentration of DMSO was 0.5% in all cases. Cytotoxicity was quantified by the MTT assay. To this end, after exposure 10 μl 5 mg/ml MTT were added to each well followed by incubation for another hour. The medium was then removed and 100 μl DMSO were added to the wells to dissolve the MTT formazan crystals. The absorbance was measured at 562 nm using a SpectraMax M2 (Molecular Devices, USA). The cell viability was expressed as % of the control, with the solvent control set at 100% viability.

2.4. DNA adduct formation

First, concentration dependent DNA adduct formation was measured in HepG2 cells for individual exposure to 0, 30,60, 90, 120, and 150 μM for 1'-OH estragole or 0, 80, 160, 200, 240 μM 1'-OH safrole. The results obtained were used to define the combined exposure regimens selecting concentrations resulting in comparable DNA adduct levels to obtain equipotent mixtures.

Secondly, to examine the interaction between the two compounds, quantification of DNA adducts was performed in HepG2 cells exposed to the individual concentrations and a mixture of 32 μM 1'-OH estragole and 200 μM 1'-OH safrole, both causing a comparable level of adduct formation from upon individual exposure.

The final concentration of DMSO in all assays was 0.1% and exposure time was 2 h. After exposure, cells from 2 T-25 flasks were harvested and collected by centrifugation at 211*g* for 5 min. The supernatant was discarded and cells were washed by resolving the pellet in 0.5–1 ml PBS followed by another centrifugation step. After final centrifugation, the final cell pellets were dissolved in 200 μl RNeasy Lysis Buffer (RLT buffer) to lyse the cells before DNA isolation.

2.5. DNA isolation and digestion

DNA isolation was performed using the QIAamp DNA Mini Kit protocol for cultured cells (Hilden, Germany). The suitable number of cells for DNA isolation was within the range of 2 $\times$ 10^6 to 5 $\times$ 10^6. After isolation, 1.5 μl of each sample was dissolved in NanodropTM One (Thermo scientific, Waltham, MA, USA) to check the concentration and purity of the isolated DNA. The purity of the isolated DNA was measured based on the absorbance ratio A260/A280 with a value of 1.8–2.0 considered as sufficiently pure. The concentration was calculated from the Nanodrop output in ng/ml using a molar extinction coefficient for double stranded DNA of 50 μg $\times$ mL^{-1} cm^{-1}. After isolation, DNA samples were freeze-dried overnight and stored at −80 °C until digestion. Dried samples were dissolved in nanopure water and adjusted to 50 μg per 30 μl before digestion. DNA digestion was performed as previously described (Yang et al., 2020a; Yang et al., 2020b). Briefly, samples were incubated with 40 μl PI-buffer (300 mM sodium acetate, 1 mM $ZnSO_4$, pH 5.3), 20 μl SPDE II solution (0.0004 U/μl in water), and 10 μl nuclease P1 (0.5 μg/μl in water) at 37 °C for 4 h. After 4 h incubation, 40 μl PA-buffer (500 mM Tris–HCl, 1 mM EDTA, pH 8.0), 20 μl VPDE I solution (0.00026 U/μl in water), and 1.6 μl AP (200 units) were added and samples were incubated at 37 °C for another 2 h.

2.6. Synthesis of major DNA adducts, and LC-MS/MS method for detection and quantification

The major DNA adducts of 1'-OH estragole N^2-(*trans*-isoestragol-3′-yl)-2′-deoxyguanosine (E-3'-N^2-dG) and 1'-OH safrole N^2-(*trans*-isosafrol-3′-yl)-2′-deoxyguanosine (S-3'-N^2-dG) were synthesized according to protocols described previously (Yang et al., 2020a; Yang et al., 2020b). LC-

MS/MS detection and quantification of these two major DNA adducts were performed also as previously described (Yang et al., 2020a; Yang et al., 2020b). In brief, LC-MS/MS analysis was performed on a Shimadzu Nexera XR LC-20 CE SR UPLC system coupled with a Shimadzu LCMS-8040 mass spectrometer (Kyoto, Japan). Samples (5 μl each) were injected onto a reverse phase C18 1.7 μm C18 100 Å, 50 × 2.1 mm column (Phenomenex, California, USA) with a column temperature at 40 °C. The gradient was made with Milli-Q water and acetonitrile both containing 0.1% (*v*/v) formic acid. The flow rate was set at 0.3 ml/min. The mobile phase was first kept at 5% acetonitrile for 1 min, and then a linear gradient was applied up to 100% acetonitrile over 5 min. The acetonitrile in the mobile phase was subsequently kept at 100% for 0.5 min, lowered to 5% in 0.1 min, and kept at the starting condition for 4.4 min. Thus, the measurement of each sample took approximately 12 min in total. Under these conditions, E-3'-N^2-dG and S-3'-N^2-dG eluted at 5.99 and 5.40 min respectively. The MS-MS analysis was carried out using a Shimadzu LCMS-8040 triple quadrupole with electrospray ionization (ESI) interface. The instrument was operated in positive mode in the multiple reaction monitoring (MRM) mode with a spray voltage of 4.5 KV. E-3'-N^2-dG was monitored at the [M+H]+ of precursor to product 414.2 → 298.2, 414.2 → 164.1, and 414.2 → 147 *m/z* at collision energy (CE) settings of 10 eV, 25 eV, and 28 eV respectively. Identification and quantification of S-3-N^2-dG was achieved at the [M+H]+ of the precursor and the transitions used for obtaining the daughter fragments which were 428.1 → 312.0, 428.1 → 164.05, and 428.1 → 161.05 *m/z* at collision energy (CE) settings of 10 eV, 25 eV and 28 eV. The level of DNA adducts was quantified using a calibration curve where the peak area of a known concentration of the synthesized DNA adduct was plotted against the corresponding DNA adduct concentration. The amount of the DNA adducts detected in the samples was related to the total amount of digested DNA in each sample, and DNA adduct levels were expressed as the number of adducts per 10^8 nucleotides (nts) based on the assumption of 1.98×10^{15} nucleotides / μg DNA.

2.7. Physiologically based kinetic modeling

In order to evaluate the potential interaction in cytochrome P450 and sulfotransferase mediated bioactivation upon combined exposure to estragole and safrole at estimated human daily intake (0.01 mg/kg bw for estragole and 0.005 mg/kg bw for safrole) (Rietjens et al., 2015; Smith et al., 2002), the maximum concentrations of estragole and safrole or their 1′-hydroxymetabolites occurring in the liver were predicted by physiologically based kinetic (PBK) modeling in humans. These concentrations were compared to the Km values for the enzymes involved in catalyzing the conversion of both parent compounds to corresponding 1′-hydroxymetabolites followed by 1′-sulfooxymetabolite formation. Given that the inhibitor could also be a substrate and converted through enzyme to product P_2, the k_3 and k_{-3} can also be considered as the k_1 and k_{-1} for this compound (Fig. 1). As Km equals $(k_{-1} + k_2)/k_1$ and Ki equals k_{-1}/k_1 it can be assumed that when the substrate concentration remains far below Km it is also likely below Ki, pointing at the absence of efficient inhibition and, thus, competitive interactions.

2.8. Data analysis

To analyze whether the response of combined exposure can be predicted by concentration addition, the cytotoxicity data were evaluated by comparison of the concentration-response curves of the individual compounds to the curve for the equivalent potency mixture expressed in 1'-OH estragole equivalents. At IC10 and IC25, the 95% confidence interval of 1'-OH estragole concentrations were calculated by GraphPad Prism 5.

The additivity for the level of DNA adduct formation was analyzed using a *t*-test to detect statistically significant differences between the added response resulting from isolated exposure and the result obtained upon combined exposure, performed by Microsoft Excel 2013 while GraphPad Prism 5 was used for plotting the data.

3. Results

3.1. Cytotoxicity upon individual and combined exposure

Cell viability of HepG2 cells was quantified by the MTT assay after 24 h of exposure to either 1'-OH estragole or 1'-OH safrole (Fig. 2). The IC50 values derived from these data amounted to 102 μM for 1'-OH estragole and 288 μM for 1'-OH safrole. Based on these results, an equipotent mixture containing 1'-OH estragole and 1'-OH safrole at a ratio of 1:3 was also tested for cytotoxicity and the result obtained, presenting cell viability as a function of the concentration expressed in 1'-OH estragole equivalents, are also present in Fig. 2. The results thus obtained show that the concentration-response curve for the combined exposure matches that of 1'-OH estragole with an IC50 value of 99 μM. Only slight deviation occurred at the lower concentrations where effects on cell viability were less than 20%. 95% interval limits for the IC10 and IC25 concentrations of the curves obtained for the combined exposure and the reference compound 1'-OH estragole revealed non statistically significant difference (data not shown). Taken together these results imply that the effects of the two compounds on cytotoxicity are additive.

3.2. DNA adduct formation upon individual and combined exposure

Fig. 3 presents the concentration dependent DNA adduct formation as detected in HepG2 cells exposed to 1'-OH-estragole or 1'-OH safrole for 2 h. In contrast to the results obtained upon 24 h exposure (Fig. 2) the concentrations tested were not cytotoxic upon 2 h exposure (data not shown). A positive linear correlation between concentration and the number of DNA adducts formed was found for both compounds (R^2 = 0.98 for 1'-OH estragole exposure and R^2 = 0.94 for 1'-OH safrole exposure). The slope of the curves reflects the ability of the respective 1'-OH metabolites to form DNA adducts and indicate DNA adduct

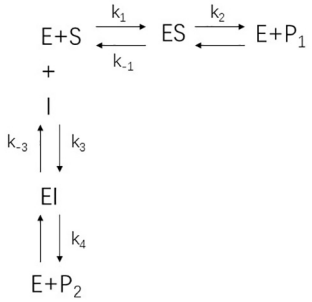

Fig. 1. Kinetic scheme for combined conversion of estragole and safrole by cytochromes P450 or combined conversion of 1'-OH estragole and 1'-OH safrole by sulfotransferases.

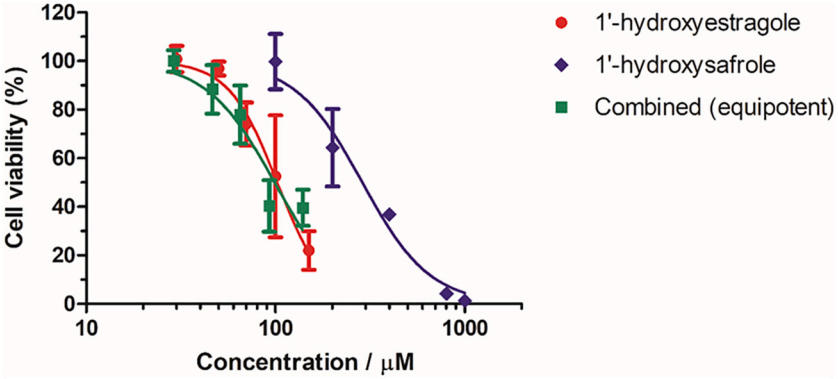

Fig. 2. Cell viability of HepG2 cells evaluated by the MTT assay after 24 h exposure to individual compounds or an equipotent mixture of 1'-OH estragole and 1'-OH safrole. Data points represent mean ± SD of three independent experiments.

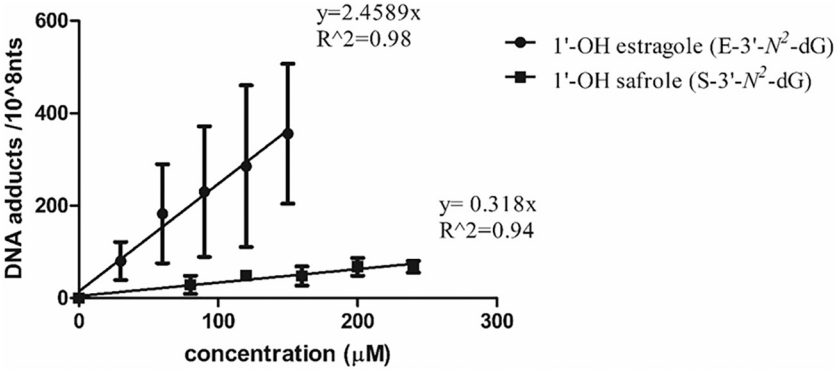

Fig. 3. DNA adduct (E-3'-N^2-dG or S-3'-N^2-dG) formation in HepG2 cells after 2 h exposure to increasing concentrations of 1'-OH estragole or 1'-OH safrole.

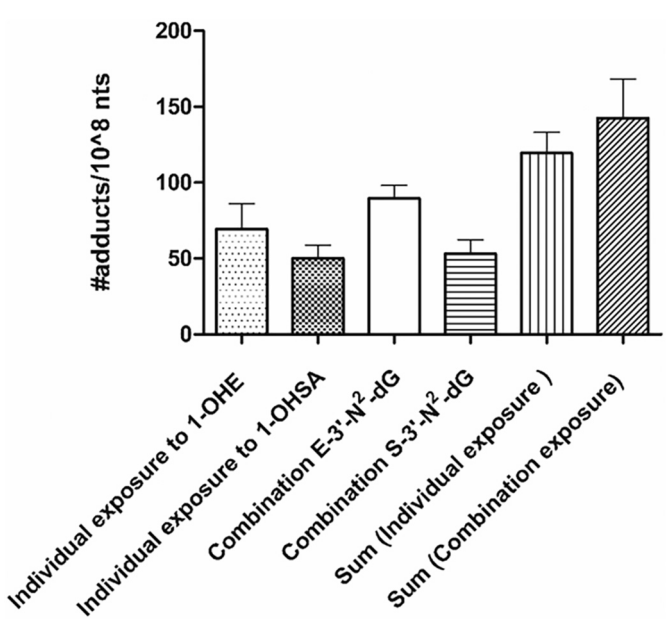

Fig. 4. DNA adduct (E-3'-N^2-dG and/or S-3'-N^2-dG) formation in HepG2 cells 2 h after individual or combined exposure to 200 µM 1'-OH safrole and/or 32 µM 1'-OH estragole. Data represent mean ± SD of three independent experiments.

formation upon exposure to an equimolar concentration of 1'-OH estragole to be higher than what is observed upon exposure of the cells to 1'OH- safrole.

To assess the DNA adduct formation upon combined exposure to these two compounds, HepG2 cells were exposed to individual concentrations and a mixture of 32 µM 1'-OH estragole and 200 µM 1'-OH safrole for 2 h, both causing a comparable level of adduct formation upon individual exposure (Fig. 4). Upon combined exposure the formation of both E-3'-N^2-dG and S-3'-N^2-dG were not statistically significantly different from the levels observed upon exposure to the compounds in isolation.

3.3. PBK modeling

The concentrations of estragole, safrole, and their 1′-hydroxymetabolites present in the liver were predicted by PBK modeling using models previously reported (Martati et al., 2012; Punt et al., 2009) at dose levels equal to the estimated daily intake of 0.01 mg/kg bw for estragole (Smith et al., 2002) or 0.005 mg/kg bw for safrole (Rietjens et al., 2015). The corresponding liver concentrations were 0.017 µM and 0.016 µM for estragole and safrole respectively (Table 1). In cytochrome P450 (CYP) mediated bioactivation, estragole and safrole share CYP2A6

Table 1
PBK model predicted concentrations of estragole, safrole, 1'-OH estragole and 1'-OH safrole in human liver upon exposure to the estimated daily dietary intake of estragole and safrole as well as the Km values for their conversion by CYP2A6 and sulfotransferases respectively.

	Estragole	Safrole	1'-OH Estragole	1'-OH Safrole
Concentration (µM)	0.017	0.016	0.04	0.005
Km (µM)	8[a]	12[a]	727[c]	3828[b]

[a] Jeurissen et al. (2007).
[b] Martati et al. (2012).
[c] Punt et al. (2007).

as a major enzyme involved in 1′-hydroxymetabolite formation (Jeurissen et al., 2007), providing a potential target for interaction upon combination exposure. In Table 1, the PBK model calculated liver concentrations are compared to the Km for this CYP2A6 mediated 1′-hydroxylation of estragole and safrole. This comparison reveals that the PBK modeling based predicted concentrations were 2 to 3 orders of magnitude below the Km for both compounds. Given that Km equals $(k_{-1} + k_2)/k_1$ or $(k_{-3} + k_4)/k_3$ and Ki equals k_{-1}/k_1 or k_{-3}/k_3 (Fig. 1) it is likely that these substrate liver concentrations are also substantially below the Ki, pointing at the absence of efficient inhibition and competitive interactions. Similar considerations hold for the sulfotransferase mediated sulfation of the 1'-OH metabolites considering the Km value and PBK model predicted liver concentrations also presented in Table 1, providing an explanation for the absence of significant interactions at the level of the DNA adduct formation in the HepG2 cells upon combined exposure to 1'-OH estragole and 1'-OH-safrole. The PBK model predicted liver concentrations of 1'-OH estragole and 1'-OH safrole amounting to 0.04 μM and 0.005 μM respectively, being also several orders of magnitude below the respective kinetic constants. Overall, these in silico results indicate that at dietary levels of intake, interactions at the level of cytochrome P450 or sulfotransferase mediated bioactivation of estragole and safrole are unlikely to occur.

4. Discussion

In this study, the consequences of combined exposure to estragole and safrole were characterized based on in vitro and in silico models. Combined effects of the proximate carcinogenic metabolites 1'-OH estragole and 1'-OH safrole for the endpoints cytotoxicity and DNA adduct formation were quantified in an in vitro cell model. Studies were performed in HepG2 cells since these cells were shown before to allow detection of the respective endpoints upon exposure to the proximate 1′-hydroxy alkenylbenzene metabolites (Yang et al., 2020a; Yang et al., 2020b). The data obtained in the present study on cytotoxicity indicate that binary mixtures of the two selected alkenylbenzene 1′-hydroxymetabolites showed concentration (dose)-addition. Interesting to observe is that the relative difference in potency between the two 1′-hydroxymetabolites for cytotoxicity was different (3fold) from the difference observed in potency for DNA adduct formation (8 fold). This may imply that the sulfotransferase mediated bioactivation, which is a determinant factor in causing 1'-OH alkenylbenzene derived DNA adduct formation, may not be the rate limiting factor in the mode of action underlying the cytotoxicity.

With respect to DNA adduct formation, also no significant interactions between 1'-OH estragole and 1'-OH safrole were observed. Such interactions could have resulted from mutual competition at the active site of the sulfotransferase catalyzing the conversion to the DNA reactive metabolites. The lack of such an interaction results from the fact that the concentrations tested for both compounds of 32 μM for 1'-OH estragole and 200 μM for 1'-OH safrole were substantially below the Km for their sulfotransferase mediated conversion reported to amount to 727 μM for 1'-OH estragole and 3828 μM for 1'-OH safrole and in incubations with human liver S9 (Martati et al., 2012; Punt et al., 2007).

In a previous study, the interaction at the level of bioactivation by CYP2A6, the major enzyme involved in 1′-hydroxylation of both safrole and estragole (Jeurissen et al., 2007; Jeurissen et al., 2004), was already considered. In this previous study PBK modeling predicted that at relatively high equimolar concentrations of safrole and estragole up to 200 μM the 1′-hydroxylation of both compounds was predicted to amount to only 52% of the total 1′-hydroxylation predicted when the interaction would not be taken into account. Given that the substrate concentration range considered in this study was substantially higher than the Km for CYP2A6 mediated conversion of safrole and estragole (Table 1), it is of interest to consider the interaction at the level of the CYPs at lower, more realistic dose levels. PBK modeling results presented in the present study indicated that at realistic estimated dietary exposure levels the concentrations of both safrole and estragole would remain over 3 orders of magnitude below the respective Km value for their conversion by CYP2A6. Therefore, the data of the present study indicate that at realistic dietary intake levels interactions between estragole and safrole at the level of the CYP mediated conversion to their proximate carcinogenic 1′-hydroxymetabolites are unlikely. The data on DNA adduct formation and sulfation of the 1′-hydroxy metabolites obtained in the present study support that also at the subsequent steps in the bioactivation interactions seem unlikely at realistic dietary exposure levels.

It should be noted that potentially interactions at the level of DNA adduct formation could also have originated from interactions at the level of repair of these adducts. However, previous studies revealed this repair to be limited and therefore unlikely to be a dominant factor for interactions (Yang et al., 2020a; Yang et al., 2020b). Furthermore, interactions at the level of detoxification of the proximate carcinogenic 1'-OH metabolites by glucuronidation and/or oxidation may also potentially play a role. However, given the results of the present study it can be concluded that also these processes do not result in detectable interactions upon combined exposure. This result is in line with the fact that the concentrations of both compounds tested were also below the Km for their glucuronidation and oxidation mediated conversions in incubations with human liver fractions reported to amount to respectively 1.32 mM and 0.55 mM for 1'-OH estragole (Punt et al., 2007), and 0.71 mM and 0.35 mM for 1'-OH safrole (Martati et al., 2012).

Finally, a previous PBK study on the potential inhibition of the SULT mediated bioactivation of estragole by the CYP inhibitor nevadensin already elucidated that, while inhibition was observed at dose levels used in rodent bioassays, the interaction was no longer observed at realistic human dietary intake levels. This is because at realistic human dietary intake systemic concentrations of the inhibitor did not reach its Ki value of 4 nM (Rietjens et al., 2015). In the present study the potential interactions at the level of both CYP and SULT mediated bioactivation were studied in silico using the previously developed PBK models in humans for estragole (Punt et al., 2009) and safrole (Martati et al., 2012).

As already indicated above, the concentrations of the parent compounds in the liver of humans upon dietary intake of the alkenylbenzenes were predicted to be orders of magnitude below the Km for the CYP mediated 1′-hydroxylation. Given that Km equals $(k_{-1} + k_2)/k_1$ or $(k_{-3} + k_4)/k_3$ and Ki equals k_{-1}/k_1 or k_{-3}/k_3 (Fig. 1), it is likely that these substrate liver concentrations are also substantially below the Ki, pointing at the absence of efficient inhibition and, thus, competitive interactions. Similar results were obtained for the predicted concentrations of the 1'-OH metabolites and the kinetic constants for their conversion by the sulfotransferase or their detoxification by glucuronosyltranferases or via their further oxidation. This explains why in the DNA adduct experiments no interaction was observed. This result is in line with the previous conclusion that interactions upon combined exposure generally mainly happen at moderate or high dose levels (Könemann et al., 1996).

In summary, the results of the present study provide support for the absence of interaction effects upon combined exposure to two selected food-borne alkenylbenzenes at dietary levels of intake. This result provides a first line of evidence to support the use of dose addition in risk assessment of their combined dietary exposure.

Author contributions

All authors contributed to the study conception and design. Ivonne M.C.M. Rietjens provided conceptualization. Shuo Yang, Tomoyuki Kawai, Sebastiaan Wesseling, and Ivonne M.C.M. Rietjens designed the experimental methods. Shuo Yang analyzed the results, and Ivonne M.C.M. Rietjens supervised the analysis. Shuo Yang wrote the first draft of the manuscript and all the authors contributed to the writing of the manuscript.

Funding

This work was supported by a grant from the China Scholarship Council (No. 201607720009) to Shuo Yang.

Declaration of Competing Interest

The authors declare no competing financial interest.

References

Alajlouni, A.M., Isnaeni, F.N., Wesseling, S., Vervoort, J., Rietjens, I.M.C.M, 2016. Level of alkenylbenzenes in parsley and dill based teas and associated risk assessment using the margin of exposure approach. J. Agric. Food Chem. 64 (45), 8640–8646.

Alajlouni, A.M., Wesseling, S., Kalli, M., Vervoort, J., Rietjens, I.M.C.M, 2017. Risk assessment of combined exposure to alkenylbenzenes through consumption of plant food supplements containing parsley and dill. Food Add. Contamin.: Part A 34 (12), 2201–2211.

Al-Malahmeh, A.J., Al-Ajlouni, A.M., Wesseling, S., Vervoort, J., Rietjens, I.M.C.M, 2017. Determination and risk assessment of naturally occurring genotoxic and carcinogenic alkenylbenzenes in basil-containing sauce of pesto. Toxicol. Rep. 4, 1–8.

Bliss, C.I., 1939. The toxicity of poisons applied jointly 1. Ann. Appl. Biol. 26 (3), 585–615.

Boberg, E.W., Miller, E.C., Miller, J.A., Poland, A., Liem, A., 1983. Strong evidence from studies with brachymorphic mice and pentachlorophenol that 1′-sulfoöxysafrole is the major ultimate electrophilic and carcinogenic metabolite of 1′-hydroxysafrole in mouse liver. Cancer Res. 43 (11), 5163–5173.

Dale, C., Garner, R., 1996. Measurement of DNA adducts in humans after complex mixture exposure. Food Chem. Toxicol. 34 (9), 905–919.

EFSA, 2012. Statement on the applicability of the margin of exposure approach for the safety assessment of impurities which are both genotoxic and carcinogenic in substances added to food/feed. EFSA J. 10 (3), 2578.

Herrmann, K., Engst, W., Appel, K.E., Monien, B.H., Glatt, H., 2012. Identification of human and murine sulfotransferases able to activate hydroxylated metabolites of methyleugenol to mutagens in salmonella typhimurium and detection of associated DNA adducts using UPLC–MS/MS methods. Mutagenesis 27 (4), 453–462.

Honda, H., Minegawa, K., Fujita, Y., Yamaguchi, N., Oguma, Y., Glatt, H., Nishiyama, N., Kasamatsu, T., 2016. Modified Ames test using a strain expressing human sulfotransferase 1C2 to assess the mutagenicity of methyleugenol. Genes Environ. 38 (1), 1–5.

Howard, G.J., Webster, T.F., 2009. Generalized concentration addition: a method for examining mixtures containing partial agonists. J. Theor. Biol. 259 (3), 469–477.

Jeurissen, S.M., Bogaards, J.J., Awad, H.M., Boersma, M.G., Brand, W., Fiamegos, Y.C., van Beek, T.A., Alink, G.M., Sudhölter, E.J., Cnubben, N.H., Rietjens, I.M.C.M, 2004. Human cytochrome P450 enzyme specificity for bioactivation of safrole to the proximate carcinogen 1 ‘-hydroxysafrole. Chem. Res. Toxicol. 17 (9), 1245–1250.

Jeurissen, S.M., Punt, A., Boersma, M.G., Bogaards, J.J., Fiamegos, Y.C., Schilter, B., van Bladeren, P.J., Cnubben, N.H., Rietjens, I.M.C.M, 2007. Human cytochrome P450 enzyme specificity for the bioactivation of estragole and related alkenylbenzenes. Chem. Res. Toxicol. 20 (5), 798–806.

Jeurissen, S.M., Punt, A., Delatour, T., Rietjens, I.M.C.M, 2008. Basil extract inhibits the sulfotransferase mediated formation of DNA adducts of the procarcinogen 1′-hydroxyestragole by rat and human liver S9 homogenates and in HepG2 human hepatoma cells. Food Chem. Toxicol. 46 (6), 2296–2302.

Könemann, W., Pieters, M.J.F., Toxicology, C., 1996. Confusion of concepts in mixture toxicology. Food Chem. Toxicol. 34 (11−12), 1025–1031.

Lévay, G., Bodell, W.J., 1992. Potentiation of DNA adduct formation in HL-60 cells by combinations of benzene metabolites. Proc. Natl. Acad. Sci. 89 (15), 7105–7109.

Martati, E., Boersma, M.G., Spenkelink, A., Khadka, D.B., van Bladeren, P.J., Rietjens, I.M.C.M., Punt, A., 2012. Physiologically based biokinetic (PBBK) modeling of safrole bioactivation and detoxification in humans as compared with rats. Toxicol. Sci. 128 (2), 301–316.

Miller, E.C., Swanson, A.B., Phillips, D.H., Fletcher, L., Liem, A., Miller, J.A., 1983. Structure-activity studies of the carcinogenicities in the mouse and rat of some naturally occurring and synthetic alkenylbenzene derivatives related to safrole and estragole. Cancer Res. 43 (3), 1124–1134.

Paini, A., Punt, A., Viton, F., Scholz, G., Delatour, T., Marin-Kuan, M., Schilter, B., van Bladeren, P.J., Rietjens, I.M.C.M., 2010. A physiologically based biodynamic (PBBD) model for estragole DNA binding in rat liver based on in vitro kinetic data and estragole DNA adduct formation in primary hepatocytes. Toxicol. Appl. Pharmacol. 245 (1), 57–66.

Punt, A., Delatour, T., Scholz, G., Schilter, B., van Bladeren, P.J., Rietjens, I.M.C.M., 2007. Tandem mass spectrometry analysis of N 2-(trans-Isoestragol-3 ‘-yl)-2 ‘-deoxyguanosine as a strategy to study species differences in Sulfotransferase conversion of the proximate carcinogen 1 ‘-Hydroxyestragole. Chem. Res. Toxicol. 20 (7), 991–998.

Punt, A., Paini, A., Boersma, M.G., Freidig, A.P., Delatour, T., Scholz, G., Schilter, B., Bladeren, P.J., Rietjens, I.M.C.M., 2009. Use of physiologically based biokinetic (PBBK) modeling to study estragole bioactivation and detoxification in humans as compared with male rats. Toxicol. Sci. 110 (2), 255–269.

Rietjens, I.M., Tyrakowska, B., van den Berg, S.J., Soffers, A.E., Punt, A., 2015. Matrix-derived combination effects influencing absorption, distribution, metabolism and excretion (ADME) of food-borne toxic compounds: implications for risk assessment. Toxicol. Res. 4 (1), 23–35.

Scientific Committee on Consumer Safety, S, Scientific Committee on Emerging and Newly Identified Health Risks, S, Scientific Committee on Health and Environmental Risks, S, 2012. Toxicity and Assessment of Chemical Mixtures. European Union, 50 pp.

Smith, R., Adams, T., Doull, J., Feron, V., Goodman, J., Marnett, L., Portoghese, P., Waddell, W., Wagner, B., Rogers, A., 2002. Safety assessment of allylalkoxybenzene derivatives used as flavouring substances—methyl eugenol and estragole. Food Chem. Toxicol. 40 (7), 851–870.

Staal, Y.C., Hebels, D.G., Van Herwijnen, M.H., Gottschalk, R.W., Van Schooten, F.J., van Delft, J.H., 2007. Binary PAH mixtures cause additive or antagonistic effects on gene expression but synergistic effects on DNA adduct formation. Carcinogenesis 28 (12), 2632–2640.

Wiseman, R.W., Miller, E.C., Miller, J.A., Liem, A., 1987. Structure-activity studies of the hepatocarcinogenicities of alkenylbenzene derivatives related to estragole and safrole on administration to preweanling male C57BL/6J× C3H/HeJ F1 mice. Cancer Res. 47 (9), 2275–2283.

Yang, S., Diem, M., Liu, J.D., Wesseling, S., Vervoort, J., Oostenbrink, C., Rietjens, I.M.C.M., 2020a. Cellular levels and molecular dynamics simulations of estragole DNA adducts point at inefficient repair resulting from limited distortion of the double-stranded DNA helix. Arch. Toxicol. 1–17.

Yang, S., Liu, J.D., Diem, M., Wesseling, S., Vervoort, J., Oostenbrink, C., Rietjens, I.M.C.M., 2020b. Molecular dynamics and in vitro quantification of Safrole DNA adducts reveal DNA adduct persistence due to limited DNA distortion resulting in inefficient repair. Chem. Res. Toxicol. 33 (9), 2298–2309.